International Journal of Nanomedicine

Dovepress
open access to scientific and medical research

Open Access Full Text Article

ORIGINAL RESEARCH

Ocular Inserts of Voriconazole-Loaded Proniosomal Gels: Formulation, Evaluation and Microbiological Studies

This article was published in the following Dove Press journal:
International Journal of Nanomedicine

International Journal of Nanomedicine downloaded from https://www.dovepress.com/
For personal use only.

Ghada Ahmed El-Emam[1]
Germeen NS Girgis[1]
Mohamed M Adel El-Sokkary[2]
Osama Abd El-Azeem Soliman[1]
Abd El Gawad H Abd El Gawad[1]

[1]Department of Pharmaceutics, Faculty of Pharmacy, Mansoura University, Mansoura, Egypt; [2]Department of Microbiology, Faculty of Pharmacy, Mansoura University, Mansoura 35516, Egypt

Background: Voriconazole (VRC) is a triazole broad spectrum antifungal drug, used in the management of versatile fungal infections, particularly fungal keratitis. The obligatory use of niosomal delivery of VRC may reduce the frequency of dosing intervals resulting from its short biological half time and consequently improve patient compliance.

Methods: VRC loaded proniosomes (VRC-PNs) were set by the coacervation technique and completely characterized. The developed formula was comprehensively assessed concerning in- vitro release behavior, kinetic investigation, and its conflict against refrigerated and room temperature conditions. A selected noisomal formula was incorporated into ocusert (VRC-PNs Ocu) formulated by 1% w/w hydroxypropyl methyl cellulose HPMC and 0.1% w/w carbopol $_{940}$. Eventually, in vitro antifungal activity against *Candida albicans* and *Aspergillus nidulans* was assessed by the cup diffusion method.

Results: The optimized VRC-PNs (Pluronic F127: cholesterol weight ratio 1:1 w/w) exhibited the highest entrapment efficiency (87.4±2.55%) with a spherical shape, proper size in nano range and a suitable Zeta potential of 209.7±8.13 nm and −33.5±1.85 mV, respectively. Assurance of drug encapsulation in nanovesicles was accomplished by several means such as attenuated total reflection Fourier-transform infrared spectroscopy, differential scanning calorimetry in addition to powder X-ray diffraction investigations. It displayed a biphasic in vitro release pattern and after 6 months of storage at a refrigerated temperature, the optimized formula preserved its stability. VRC-PNs Ocu proved a very highly significant antifungal activity matched with the free drug or nanosuspension which was extra assured by comparing its mean inhibition zone with that of 5% natamycin market eye drops.

Conclusion: In conclusion, VRC-PNs Ocu could be considered as a promising stable sustained release topical ocular nanoparticulate system for the management of fungal infections.

Keywords: voriconazole, proniosomes, coacervation, ocusert, antifungal activity

Introduction

The progression of an optimum topical ocular drug delivery is, up till now, a problematical mission for formulation scientists owing to the complicated anatomical, physiological and formulation limitations.[1,2] Furthermore, cornea with hydrophilic stroma sandwiched between the lipophilic epithelium and endothelium limits the permeation of hydrophilic and lipophilic drugs deep through the eye.[3]

Alongside various protective ocular barriers such as; lacrimation, reflux blinking and nasolacrimal drainage, short pre-corneal residence and deprived corneal penetrability are

Correspondence: Germeen NS Girgis
Department of Pharmaceutics, Faculty of Pharmacy, Mansoura University, Mansoura 35516, Egypt
Tel +2 01200960016
Fax +20 (50) 239733
Email g.girgis2012@yahoo.com

submit your manuscript | www.dovepress.com
DovePress
http://doi.org/10.2147/IJN.S268208

© 2020 El-Emam et al. This work is published and licensed by Dove Medical Press Limited. The full terms of this license are available at https://www.dovepress.com/terms.php and incorporate the Creative Commons Attribution – Non Commercial (unported, v3.0) License (http://creativecommons.org/licenses/by-nc/3.0/). By accessing the work you hereby accept the Terms. Non-commercial uses of the work are permitted without any further permission from Dove Medical Press Limited, provided the work is properly attributed. For permission for commercial use of this work, please see paragraphs 4.2 and 5 of our Terms (https://www.dovepress.com/terms.php).

the vital dynamics responsible for reducing the bioavailability (<5%) of instilled conventional ophthalmic preparations.[4,5]

Various nano-strategies such as solid lipid nanoparticles (SLN), nanostructured lipid carriers (NLC), polymeric nanoparticles, micelles, nanoemulsions, liposomes besides noisomes and phospholipid have been succeeded in improving the transcorneal drug penetrability.[6,7]

In ophthalmic vesicular drug delivery systems comprising liposomes and noisomes, mutual enhancement of the bioavailability as well as drug accumulation is manifested via encapsulation of the drug in lipid vesicles allowing its penetration across cell membrane and therefore, prolonging the extent of action at the corneal surface.[8]

Proniosomes are either anhydrous free- flowing preparations "dry niosomes" or liquid crystals with jellylike consistency of water-soluble carrier covered with the appropriate surfactants which can be rehydrated on prerequisite with gentle shaking at a temperature greater than the mean transition phase temperature of the surfactant to give conventional noisomes of uniform size. They are preferred over noisome, because of physical stability through avoiding aggregation, fusion or leakage; beside the ease of preparation; and also they are cheaper and more stable against oxidative hydrolysis than liposomes.[9]

Azoles have antifungal activity by blocking the P450 (CYP)-dependent 14α sterol demethylase enzyme, which is responsible for the synthesis process of ergosterol from lanosterol and accordingly disturbs cell membrane of fungi. In this way, they permit the accumulation of toxic methyl sterols in the fungal cell membrane and retard the growth and replication of fungal cells.[10] However, the famous adverse effects of the majority of azoles include visual disturbances, hepatic deformities in addition to drug interaction profiles, which are attributed to cross-inhibition of different CYP-dependent enzymes.

Voriconazole (VRC) structure [(2R, 3S)-2-(2, 4-difluorophenyl)-3-(5-fluoropyrimidin-4-yl)-1-(1H-1, 2, 4-triazol-1-yl) butan-2-ol)] is a potential antifungal drug belonging to azole group. It is a lipophilic drug (Log P 1.65) with low pH- dependent aqueous solubility 0.5–0.71 mg/mL at neutral pH (maximum 2.7 mg/mL at pH 1.2).[11] VRC is classified as a BCS class II (Biopharmaceutics Classification System),[12] highly potent drug at a concentration ≤1 mg/ L against resistant fungal species including *Fusarium, Scedosporium apiospermum, Cryptococcus neoformans, Coccidioides, Blastomyces, Histoplasma*, fluconazole-resistant *Candida* species. Moreover, it has now become the prime treatment for aspergillosis associated with keratitis.[10]

VRC is only marketed as an oral and intravenous preparation with excellent bioavailability. Promising results have been achieved using voriconazole drops which were prepared through Vfend powder reconstitution in numerous scientific studies that have established the essential role of topical inventions. In a study,[13] after intracameral injection of 1% voriconazole, effective treatment of corneal ulcers with a coinfection of acanthamoeba and fungal organisms was recognized with its ability to prevent recurrence of both. To date, no topical ocular formulation containing VRC has become available in the market even though numerous efforts involving cyclodextrinbased eye drop solutions and gels,[14,15] microemulsions,[16] liposomes,[17] and noisomes[18] have assured the prospective request for VRCbased topical eye products. Several works of literatures have reported the high intraocular penetration of topical VRC with concomitant therapeutic concentration that can be attained in different eye tissues with proven effectiveness against fungal keratitis.[19,20]

Regarding the short biological half-life of VRC, which necessitates multiple daily dosing, there is an obligate requirement for a novel delivery system such as niosomal delivery, as a means for reducing the frequency of dosing intervals and enhancement of patient compliance. Previous preparation of VRC encapsulation as noisomes by hand shaking and ether injection method by using span 80 and cholesterol had been detailed.[21]

Fungal keratitis is a worldwide-distributed ocular infection caused by various fungi. The main etiology of this disease varies based on geographical origin, socioeconomic status, and climatic conditions. Generally, *Aspergillus* spp. and *Fusarium* spp. are common in tropical and subtropical regions and *Candida* spp. are dominant in temperate areas.[22,23] The reported in vitro minimum inhibitory concentrations of VRC in case of *Aspergillus* spp. and *Candida* spp. were 0.5 and 0.016 (μg/mL), respectively.[24]

Antifungal susceptibility testing is accomplished to afford appropriate data for clinicians to choose a suitable antifungal agent that is beneficial for overcoming a certain fungal infection. Several methods have been utilized for susceptibility study of different fungal species to fungicidal drugs for example; broth macro and micro dilutions at which several dilutions for each drug by the addition of the drug powder to Muller Hinton Broth were made, agar dilution, E-test (MICs readings were accomplished by the

aid of E-test guide), sensitive colorimetric microdilution panels where a dye was added to the dilutions of the drugs and disk diffusion where antifungal discs of different antifungal drugs were applied.[25] In our study, we will focus on the cup diffusion method.

The intention of this study was to ascertain the possible use of the proniosomes laden ocular inserts as nanocarriers for the ocular delivery of voriconazole with improved antifungal activity.

Materials and Methods

Materials

VRC was friendly provided by Pfizer pharmaceutical company, Egypt. Cholesterol, Span 60 (sorbitan monostearate), Span 80 (sorbitan monooleate) and pluronic F 127 (poloxamer 407) were obtained from Sigma-Aldrich Co. (St. Louis, MO, USA). Ethyl alcohol, Tween 80, Disodium hydrogen phosphate, and Potassium dihydrogen orthophosphate were acquired from El Nasr pharmaceutical company (Cairo, Egypt). Spectra/Pore® dialysis sheath (12,000–14,000 molecular weight limit) was obtained from Spectrum Laboratories Inc (Los Angeles, CA). The market eye drops Natacyn® containing a sterile suspension of natamycin 5% manufactured by Alcon-Couvreur (Belgium) was bought to be employed in our studies.

Methods

Preliminary Screening of the Optimal Circumstances for Preparation of (VRC-PNs)

With the aim of the better surfactant choice to be investigated in the preparation of VRC-PNs, four different surfactants were estimated. Pluronic F127 and tween 80 are representative of high hydrophilic- lipophilic balance "HLB" surfactants (HLB = 18 and 15, respectively), while Span 60 and Span 80 as descriptive of surfactants with low HLB values (4.7 and 4.3, respectively). Also, cholesterol amount was used in three different weight ratios relative to the surfactants used; 1:1, 2:1 and 1:2.

The effect of changing those two variables on particle size, uniform distribution (PDI), surface charge (ZP) and loading efficacy percentage (EE %) of the formed noisomes was examined. Twelve formulae were prepared and fully characterized. Their compositions are represented in Table 1.

Preparation of VRC-PNs by Adopting Coacervation Phase Separation Technique

Proniosomes were formed by the coacervation phase separation process reported earlier.[26–28] Precisely weighed quantities of cholesterol, individual surfactant, and VRC for each formula were properly agitated with 0.8 mL of absolute ethyl alcohol in a small stoppered glass vial. The glass vial was immersed in a water bath at a temperature of 70–80°C for 5 min with continuous stirring until the dispersion of lipids was achieved. Then, the addition of preheated 0.2 mL of deionized water to the molten blend was required, while agitation was continued in the water bath for an extra 3 min till monophasic mixture was attained. White creamy proniosomal gel was obtained when the mixture left-hand to turn cold to room temperature. When required, the proniosomal gel is reconstituted with deionized water, stirred for 2 h and sonicated to get freshly prepared VRC-loaded niosomal suspension.[9]

Table 1 Composition of the Different Prepared VRC-PNs

Formulation*	Span 80	Tween 80	Pluronic (F127)	Span 60	Cholesterol
F1	250 mg				250 mg
F2	250 mg				500 mg
F3	500 mg				250 mg
F4		250 mg			250 mg
F5		250 mg			500 mg
F6		500 mg			250 mg
F7			250 mg		250 mg
F8			250 mg		500 mg
F9			500 mg		250 mg
F10				250 mg	250 mg
F11				250 mg	500 mg
F12				500 mg	250 mg

Note: *Each formulation contains 10 mg VRC.

Characterization of VRC-PNs Consequential Noisomes

Each proniosomal gel formulation is reconstituted with deionized water to form 25 mL of VRC-loaded niosomes. The obtained niosomes are then extra characterized.

Estimation of Entrapment Efficiency Percent (EE %) of VRC-PNs

EE % was estimated by the direct method after centrifugation of each niosomal suspension at 13,000 rpm for 90 min at 4ºC using cooling ultracentrifuge (CE16-4X100RD, ACCULAB®, USA). The precipitated cake was appropriately dissolved and diluted with ethanol followed by spectrophotometric estimation of the entrapped VRC quantity (model UV-1601 PC, Shimadzu, Kyoto, Japan) at predetermined λ_{max} =256 nm using a blank of corresponding plain PNs treated by the same way. Drug EE % was determined conferring to the subsequent equation:[29]

$$EE\% = \frac{\text{Amount of entrapped VRC}}{\text{Total amout of VRC}} \times 100 \qquad (1)$$

Assessment of Particle Size, Polydispersity Index (PDI) and Zeta Potential

These properties were measured by Malvern Zetasizer (Malvern Instruments Ltd., Worcestershire, UK) by the application of Dynamic Light Scattering (DLS) and laser doppler microelectrophoresis strategies. This was accomplished through dilution of the niosomal dispersions in the ratio of (1:10) with deionized water and sonication by an ultrasonic bath (Sonix USA, SS101H230) to obtain uniformly distributed noisomes.

Transmission Electron Microscope (TEM) Imaging

One drop from the fresh, optimized niosomal dispersion (F7) after dilution was appropriately adsorbed on carbon covered copper lattice. After this, extra dispersion was removed by a filter paper, and then left to dry for 10 min at ambient conditions and examined without staining. Image was capture and screening of morphological characteristics via TEM (Joel JEM 1400, Tokyo, Japan) was performed.

Attenuated Total Reflection Fourier-Transform Infrared (ATR- FTIR) Spectroscopy

ATR- FTIR spectra of VRC, Pluronic F 127 "PLu F127", cholesterol CH, physical mixture PM, plain F7, and VRC-F7 Ns were studied by means of an ATR- FTIR-8400 (Thermo Fisher Scientific iS10 Nicolet Model, U.S.A). Scanning over a wavenumber range of 4000–400 cm-1 was performed for a small amount of each sample approximately 2–3 mg.

Differential Scanning Calorimetry (DSC)

The adjusted formulation, besides its plain one was frozen for 24 h then, freeze-dried at −45 ºC under $7x10^{-2}$ mbar pressure using a lyophilizer (Labconco (LYPH.LOCK 4.5)-USA).[30] A record of the corresponding DSC thermograms for individuals (Shimadzu DSC 50; Kyoto, Japan) was assessed. A sample (3–4 mg) was placed on the aluminum pan with a flat bottom and heated at a constant rate of 10ºC/min, over a temperature range of 25–300ºC, under a flow of nitrogen gas at a rate of 30 mL/min.

X-Ray Diffractometry (XRD)

X-ray diffractometer (Diano, Woburn, MA, USA) equipped with Cu Kα was utilized to establish the X-ray diffraction pattern of VRC, PLu F127, cholesterol CH, physical mixture PM, plain F7, and VRC-F7. The equipment was adjusted at 9 mA and 45 kV with a scanning range from 3º to 50º and an angle of 2θ.

Preparation and Physicochemical Evaluation of VRC-PNs Ocu

Ocular inserts incorporated with niosomal dispersion of F7 in a concentration equivalent to (1% w/w) were prepared according to the film casting method.[31] Carbopol $_{940}$ (0.1% w/w) was used in combination with hydroxypropyl methyl cellulose HPMC to enhance the elasticity, film properties, and bioadhesion. The addition of 10% propylene glycol is required as a plasticizer, which helps in the formation of flexible films.

Triethanolamine (TEA) was added to allow CP_{940} gelation and sonication for 1 h in an ultrasonic water bath and then it was stored for 24 h at ambient temperature for complete hydration. Then, 30 g of the formed solution was transmitted into Teflon plates. The solvent was permitted to evaporate for 72 h at room temperature. Each formed film was weighed and transferred to a desiccator containing silica gel, where it was stored for another 24 h before use. The prepared ocuserts were cut in the shape of circular discs, 10 mm in diameter. Then, they were individually sealed in foil sachets until further studies.

Thickness Determination

Thickness of different inserts was recorded at diverse places on the plate by means of a digital micrometer screw gauge (Mitutoyo, Japan) and mean film thickness was recorded.

Weight Uniformity

Ocular inserts were taken from different areas of the film and weighed individually. The average weights of inserts were calculated.

Drug Content

The ocular inserts from different regions of the film were taken. Drug content was estimated by dissolving the ocular insert in 50 mL of phosphate buffer pH 7.4 containing 10% ethanol with the help of stirring. The solution was clarified over filtration by Millipore filter and drug content was determined by UV–Visible spectrophotometer at predetermined λ_{max} =256 nm using a blank of the corresponding plain ocular insert.

pH Determination

One ocular insert was mixed with 10 mL distilled water with a homogenizer, then the readings were taken in triplicates by means of a digitalized pH meter (Beckman Instruments Fullerton, CA 92634, Germany).

In-Vitro Release

The in-vitro release of VRC from optimized niosomes F7 with (CH: PLu F 127 1:1) was compared to drug suspension in water as a control. In addition to this, VRC-PNs Ocu were compared with free drug -loaded ocusert. The formulae were placed in a horizontal GFL shaking water bath (GFL, Gesellschaft fur Labortechnik GmbH, Burgwedel, Germany), adjusted at a 100 rpm agitation speed and 37± 0.5ºC temperature. Several cells encompassing 70 mL of the medium of release, which was phosphate pH 7.4 containing 0.25% w/w tween 80, were placed in the shaker whereas, two milliliters of the tested formula (equivalent to 1 mg of drug) was loaded over a presoaked dialysis membrane and occluded using a parafilm.

At prearranged time intermissions, aliquots of 2 mL were withdrawn from the release medium and exchanged with an equal volume of auxiliary release medium to retain a sink condition.[27]

Spectrophotometric assay to assess the percentage of VRC released at each time interval was conducted at the preset λ_{max} (261 nm) consuming phosphate buffer with 0.25% w/w tween 80 as a blank and the percentage of the cumulative amount released from the drug at each time was calculated through the subsequent equation;[32]

$$Qn = \frac{Cn \times Vr + \sum_{i=1}^{n-1} Ci \times Vs}{initial\ drug\ amount} \quad (2)$$

Where;

Q_n: Present cumulative percent of drug released

C_n: The receptor medium present concentration at n^{th} sample

V_r: Volume of receptor medium

V_s: Volume of each sample detached for examination

$\sum_{i=1}^{n-1} Ci$: Sum of the earlier concentrations.

Release Kinetics

Release information developed from different formulae was kinetically analyzed by means of GraphPad Prism software (version 6.00; Graphpad software, San Diego, CA, USA). Generally, the analysis of in vitro release data was tailored to zero-order, first-order, and diffusion-governed release models.[33] For supplementary evaluation, the release mechanism, Korsmeyer–Peppas kinetic model, was manifested to aid in the precision of the main transport mechanism.[34] The model presenting the maximum correlation coefficient (R^2) was advised to describe VRC release pattern of different formulae.

Stability Study

The packing stability of the designated niosomal suspension F7 displaying the uppermost drug encapsulation was evaluated over 6 months at refrigerated temperature (4±1° C) besides ambient temperature (25°C±1°C) by storage in glass vials sealed with aluminum foil. Then it was kept under two different conditions. Investigation of EE %, size distribution, PDI and ZP at the beginning (0 month) and at every month during the storage period should be recorded.[35]

Microbiological Study of VRC-PNs Ocu Determined by Performing of Antifungal Susceptibility Test

Plate Microbioassay (Agar Cup Diffusion) Method

The assay was performed with cultures of *Candida albicans* (SC5314),[36] and *Aspergillus nidulans* (13962) (Eidam) G. Winter isolated by (Mycological Center, Assiut, Egypt, 71516) on sabaroud dextrose agar (SDA) fortified with levofloxacin antibiotic to guard against bacterial growth; then these SDA recovered isolates were subcultured with yeast extract 10 g, peptone water and 20 g and dextrone 20 g (YPD) and incubated at 28°C for 3 days for sporulation improvement. Following this,

microscopic examination was performed, and the growth was harvested in SDA of thickness 3–4 mm.

Cups of 10 mm diameter were punched out via a steel borer, even streaking through a sterile cotton swab that was immersed into the inoculum suspension in case of *Candida albicans* plates while homogenous seeding was performed in case of *Aspergillus nidulans* plates. An aliquot of 50 µL of our examined samples (drug suspension and niosomal suspension) as well an ocusert containing free drug and VRC-PNs Ocu in a concentration 1% w/w VRC after appropriate wetting with sterile water for injection were employed in different cups in triplicate plates for each species. Mean diameters of zone of inhibition (ZI) for *Candida albicans* and *Aspergillus nidulans* were measured after 24 h and 72 h incubation at 25°C for 24 h, correspondingly. Each type of sample was tested in triplicate. Following this, the interpretation of zone diameters was done consistent with the Clinical and Laboratory Standards Institute CLSI 2009 rules.[37]

Comparative Antifungal Susceptibility Test

Various concentrations of VRC ocuserts were prepared, which included 0.5mg, 0.75mg and 1mg/an ocusert, respectively. SDA was employed for the in-vitro antifungal sensitivity test of fungal isolates. The zones of inhibition ZI were recorded and compared with control natamycin 5% antifungal eye drops.

Statistical Study

One-way variance exploration monitored by Tukey–Kramer and Dunnett's multiple comparisons test as well Student t-test were useful to accomplish statistical assessment of the outcomes at points of significance $\rho < 0.001$ and $\rho < 0.05$. This analysis was completed by means of the GraphPad Prism software.

Results and Discussion

Characterization of Different Niosomal Formulations

Along with the primary assessment, the greatest acceptable circumstances for vesicle preparation were: VRC at an amount of 10 mg, use of ethanol as an organic solvent, and deionized water for hydration. The formation of the vesicles is welldefined subsequent to hydration and stirring for 2 h.

Table 2 represents the different nano- size ranges, dispersibility, Zeta potential and entrapment efficiencies of all prepared formulations.

As shown, particle size ranged from 193.2±7.63 to 532.3±12.88 nm, PDI of all formulations were relatively low not exceeding (0.31) while, EE % was in the range of 36.9±4.44% to 87.4±2.55%. Moreover, the Zeta potential ranged from −18.4±3.12 to −51.3±2.11 mV. Furthermore, the weight ratio of cholesterol to the surfactant that achieved the highest EE % for each surfactant used was 1:1.

Effect of Type of Nonionic Surfactants

Nonionic surface-active agents SAA are the most famous type used in formulating vesicles attributable to their properties concerning stability, compatibility, less toxicity, less hemolytic, being less cellular surface irritation and physiological pH maintenance.[38]

Table 2 Physical Evaluation of the Different Prepared VRC-PNs

Formulation Code	Weight Ratio	Parameter (Mean ±SD, n=3)			
		Particle Size (nm)	PDI	Zeta Potential (mV)	EE %
F1	CH 1:1 Sp80	415.9±10.12	0.272±0.05	−45.9±3.41	42.3±3.62
F2	CH 2:1 Sp80	315.5±8.33	0.071±0.09	−51.3±2.11	36.9±4.44
F3	CH 1:2 Sp80	441.7±6.19	0.291±0.11	−37.2±3.63	32.4±2.91
F4	CH 1:1 Tw80	520.1±4.15	0.228±0.13	−18.4±3.12	62.8±4.23
F5	CH 2:1 Tw80	480.2±5.51	0.171±0.05	−22.6±1.92	50.9±5.11
F6	CH 1:2 Tw80	532.3±12.88	0.222±0.02	−24.9±2.24	45.7±3.14
F7	CH 1:1 PLu F127	209.7±8.13	0.193±0.01	−33.5±1.85	87.4±2.55
F8	CH 2:1 PLu F127	193.2±7.63	0.231±0.04	−31.8±2.99	81.5±2.41
F9	CH 1:2 PLu F127	245.4±3.98	0.270±0.03	−34.2±3.52	78.3±1.66
F10	CH 1:1 Sp60	323.6±6.41	0.172±0.06	−38.1±2.66	77.4±2.18
F11	CH 2:1 Sp60	301.8±12.63	0.185±0.05	−34.9±2.82	67.6±3.17
F12	CH 1:2 Sp60	402.9±9.72	0.310±0.02	−31.7±1.17	54.3±2.42

Notes: Each value represents the mean ± SD (n=3); Each formulation contains 10 mg VRC.
Abbreviations: EE, entrapment efficiency; PDI, polydispersity index; CH, cholesterol; Sp80, span 80; Sp60, span 60; Tw80, tween 80; PLu F127, pluronic F127.

The surfactants' HLB is an important parameter in their choice as it affects their ability to form nanoparticles.[39] High HLB value of tween 80 results in a reduction of surface free energy producing larger vesicles.

It is clear that the order of EE % from different formulae by using diverse surface active agents SAA is as follow; PLu F127< Sp 60 <Tw 80 < Sp 80. The encapsulation efficiency of Tw 80 and Sp 80 containing vesicles are relatively low as compared to Sp 60 containing noisomes.

The lower entrapment efficiency of Sp 80 formulations, ranging; from 77.4±2.18% to 42.3±3.62% for F10 (CH1:1Sp 60) and F1 (CH1:1Sp 80), respectively, despite the similarity between Sp 60 in the alkyl chain carbon atoms (C18) and nearly matched HLB values, is mostly linked to the existence of double bonds in the alkyl chains of Sp 80. This is attributable to the increase in the permeability of the niosomal bilayer for the entrapped drug as the packing of the adjacent molecules may not be tight and consequently, the EE % decreased.[38]

The transition temperature of surfactants also affects the entrapment of drug in vesicles. Surfactants with high phase transition temperatures provide high entrapment for the drug and vice versa.[40,41] The fact that PLu F127 and Sp 60 exhibit high EE % was ascribed to various causes for instance; being solid at room temperature with positive phase transition temperature (Tc=25ºC and 53ºC, respectively). This is the main reason for further involvement in more rigid bilayers, reducing drug leaching from the vesicles; therefore improving entrapment efficiency.

In addition, pluronics retard the drug leakage by a suggested mechanism as they may be adsorbed on cholesterol membrane; stabilize the vesicles via discriminatory incorporation into low lipid density regions of the membrane, as a result of which, firmly packed lipids constituting the drug are formed.[42]

The lower entrapment efficiency of Tw 80 in relation to Sp 60 formulations may be as a result of Tw 80 hydrophilicity with HLB value greater than that of Sp 60 (HLB =15 compared to 4.7).

Effect of Cholesterol to Surfactant Ratio

Cholesterol "CH" is a vital amphiphilic component of noisomes. Cooperation of CH with a surfactant to construct hydrogen bonding among its hydroxyl groups with a hydrophilic head of the surfactant influences vesicle stability, the mechanical rigidity of vesicles and membrane cohesion, the leakiness of membrane and finally increases the entrapment efficiency of noisomes. The addition of cholesterol enables more hydrophobic surfactants to form bilayered vesicles, suppresses aggregation and provides better lipid bilayer firmness.[35,43]

Consequently, the addition of water leads to swelling of the bilayer owing to the interaction between water and the polar groups of the surfactants, leading to the formation of multivesicular, multilamellar and spherical shaped structures.[44]

From the previously shown results in Table 2, it was found that varying cholesterol: surfactant ratio from 1:2 (w/w) to 1:1 (w/w) led to a significant increase in EE % as in F1, F4, F7 and F10 which might be due to the fact that as cholesterol increases, the rigidity increases and lipophilicity as well as permeability of the bilayer decrease, fabricating efficient entrapment of the lipophilic drug into bilayers as vesicles formed. On the other hand, it was likewise observed that very high cholesterol content had a depressing effect on drug entrapment in the vesicles as in formulae where the ratio of cholesterol: surfactant is 2:1 (w/w); for F2, F5, F8 and F11. This may be due to greater quantities of cholesterol beyond a certain limit that may coincide with the drug to block the pores inside the bilayer, which accordingly causes a disturbance in the structural regularity of vesicular sheaths and also decreases the entrapment efficiency.

Regarding the particle size, the analysis clarified the increase in the niosomal vesicle size associated with a decrease in CH ratio of the formulations. Thus, the decrease in particle size in a ratio 1:1 (w/w) rather than 1:2 (w/w) can be attributed to the augmented interactions of cholesterol and the hydrophobic tail of surfactant, leading to adjacent stuffing of the bilayers in the noisomes. Similar findings were also observed by other researchers.[45,46]

Regarding ophthalmic drug delivery systems, smaller particles less than 1μm are marked with a great surface area, less eye irritation, thereby improving the corneal permeability and prolonging the mean ocular residence time.[47,48]

Table 2 demonstrates that PDI values of all the tested formulae were in the range of 0.071–0.31, thus indicating a unimodal normal symmetrical frequency distribution pattern and good homogeneity.

PDI is useful for estimation of the average dispersion homogeneity, and higher PDI values correspond to a larger size distribution in the dispersed sample. The low PDI (0.1–0.25) displays a monodispersed or a narrow size distribution,[49] while, PDI over 0.5 indicates a wide size distribution and more polydispersion.[50]

Zeta potential is a measure of net charge on a niosomal surface. As the charge on the surface of noisome decreases, the repulsive force between the vesicles also decreases, which may lead to aggregation of the vesicles.[51]

Agglomeration causes instability may be due to uneven distribution of suspension as a result of low repulsive forces, which provides a faster settling rate.

As summarized in Table 2, Zeta potential values for VRC-Ns ranged from −18.4±3.12 to −51.3±2.11 mV, showing that the organized noisomes possess sufficient charge to prevent their accumulation due to electrical repulsion. Generally, Zeta potential values around ±30 mV signify steady nano-sized systems.

Consequently, the optimum niosomal formula which would be therapeutically effective for topical delivery of VRC as an antifungal agent, is F7 (CH 1:1 PLu F127) as represented by the appropriate size of 209.7±8.13 nm, PDI 0.193±0.01, and Zeta potential −33.5±1.85 mV as illustrated in Figure 1 and maximum EE % of 87.4±2.55%. Hence, F7 was selected for further investigations.

Transmission Electron Microscopy Examination

Figure 2 clarifies the TEM microimage of the niosomal formula (F7). It has a nearly spherical shape with a smooth surface showing that encapsulated drug vesicles are in nano–size range with no signs of aggregation, signifying the physical stability of the produced nanoemulsion.

ATR- FTIR Spectroscopy

In order to examine possible interactions between VRC and pluronic F127 as well as with cholesterol, FTIR spectroscopy studies were performed.

FTIR spectra of the VRC powder, pluronic F127 powder, cholesterol powder, physical mixture, plain F7 and medicated F7 are displayed in Figure 3A. The VRC powder spectrum (i) revealed an absorption peak at 666 cm^{-1} of N (2), N(4), coordination mode of 1H,1,2,4-triazole,[52] and peaks at 3202 cm^{-1} and 3123 cm^{-1}corresponding to the stretching vibrations of OH and aromatic rings, respectively. The bands at 2980–2883, 1600–1460, and 1589–1620 cm^{-1} were assigned to the C = C aromatic, alkane CH, and aryl C-N stretches, respectively.

The IR spectrum of PLu F127 (ii) is categorized by main absorption peaks at 2882 cm-1 (C-H stretch aliphatic), 1342 cm^{-1} (in-plane O-H bend) and 1111 cm^{-1} (C-O stretch), that were consistent in the physical mixture with the drug.[53]

Pure CH peaks (iii), which were observed at 3421 cm^{-1}, corresponded to symmetric stretching of hydroxyl groups, whereas the frequency at 2935 cm^{-1} attributed to the strong

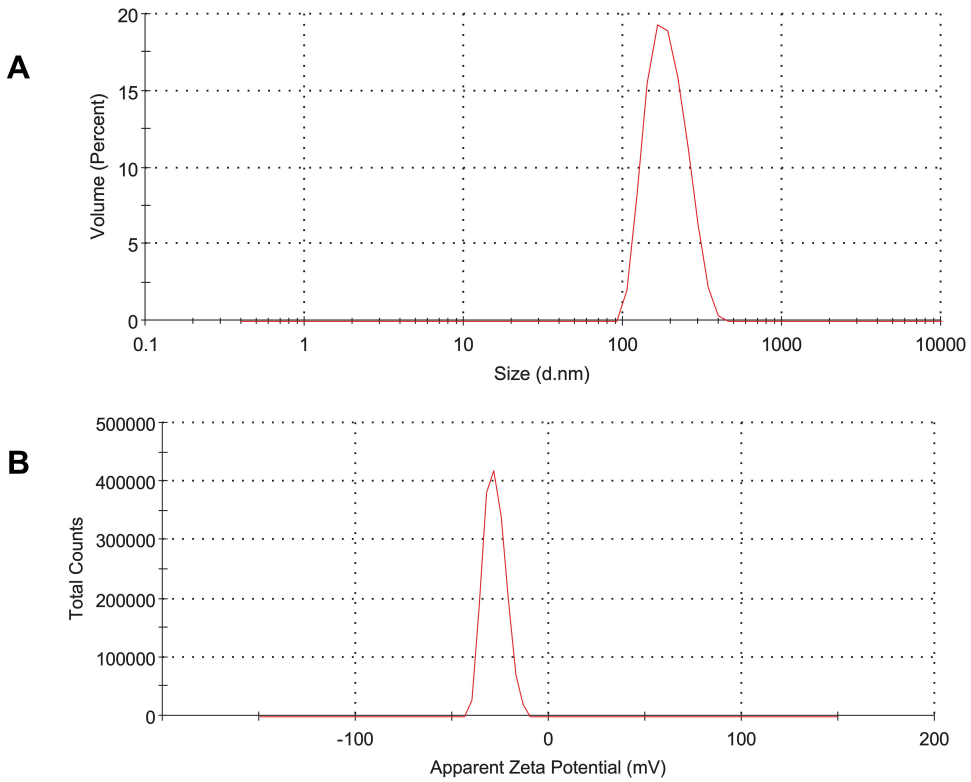


Figure 1 (**A**) Size distribution curve, and (**B**) Zeta potential distribution curve of VRC- Ns (F7).

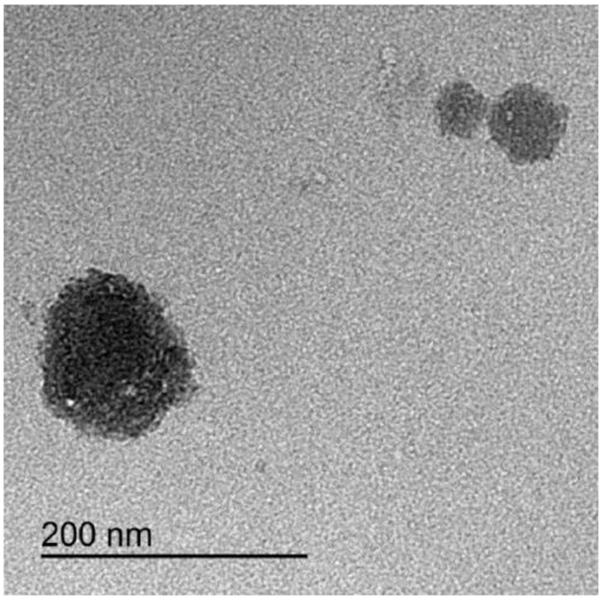


Figure 2 TEM images of optimized F7niosomal suspension.

aromatic stretching of CH=CH; while 1744 cm^{-1} was due to the strong C=O of the carboxylic group.

ATR-FTIR spectra of physical mixture PM (iv) show similar peaks as in the individual spectrum of pure ingredients. No appearance or disappearance of the distinctive bands of VRC after mixing, represents the absence of any chemical interaction between VRC and the ingredients used.

The optimized noisome formulation VRC F7 displayed only the typical bands of PLu/CH, indicating that free VRC cannot be detected in the sample. This might actually indicate that VRC was completely included in the nanovesicles; however, disappearance of the distinguishing band of VRC (3202 cm^{-1}) can be clearly observed in F7 spectrum (vi).

The modification in the intensity of the FTIR peaks of VRC F7clearly indicates the presence of a hydrogen bond interaction between the drug and other niosomal components; which mirrored the increase in drug dissolution and the existence of the drug in an amorphous state that is in agreement with reported findings in the literature.[54]

Powder X-Ray Diffraction (PXRD)

Diffraction patterns of free VRC, PLu F127, CH, physical mixture (PM) and F7 are illustrated in Figure 3B. The diffraction spectrum of VRC alone (i) shows the high drug crystallinity related to the existence of sharp peaks

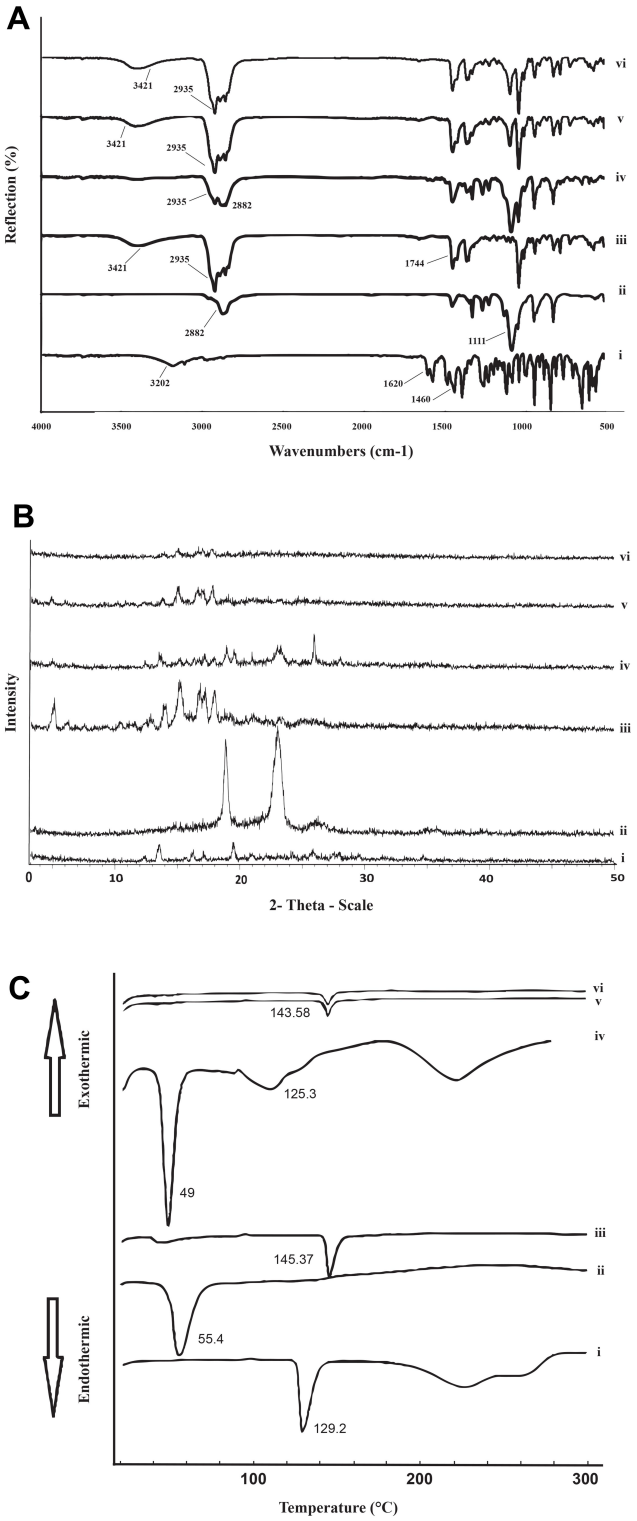


Figure 3 Solid characterizations.

Notes: (**A**) ATR- FTIR spectra, (**B**) XRD pattern and (**C**) DSC curves of (i) VRC, (ii) PLu F127, (iii) cholesterol, (iv) physical mixture, (v) plain noisomes and (vi) VRC noisomes.

Abbreviations: PLu F127, pluronic F127; ATR- FTIR, attenuated total reflection Fourier transform infrared spectroscopy; DSC, differential scanning calorimetry; XRD, X-ray diffractometry.

at 2θ values of 12.35°, 13.53°, 16.23°, 17.11°, 19.49°, 20.95°, 25.88°, 27.79° and 34.15°.[55]

As shown in (ii), PLu spectrum has three characteristic strong peaks at 2θ = 19.04°, 23.20° and 26.37°.

Figure 3B (iii) displays the PXRD of cholesterol with sharp peaks at 2θ values of 5.26, 13.00°, 14.16°, 15.37°, 16.93° and 17.35°.

The PXRD of the physical mixture in a ratio of (1:1) shows the noticeable crystalline peaks of both the drug and carriers with lower intensities (iv) indicating that the crystalline drug structure remained unchanged during physical mixing.

Powder X-ray diffraction of the freeze-dried Ns containing VRC F7 (vi) shows only the peaks that parallel to the diffraction outline of CH only; whereas, the representative peaks of VRC entirely disappeared.

These findings indicate that the drug is completely entrapped in the vesicular system and transformed into an amorphous state that has a higher internal energy and molecular motion than the crystalline one in the proximity of lipid excipients. The transition from the crystalline to an amorphous state is known to augment the free energy of the drug molecules in the system and decrease the drug melting point. Consequently, the amorphous state enhances the solubility and the dissolution rate of the drug.[11] Similar findings were earlier conveyed for other drugs loaded in niosomal systems.[56,57]

Differential Scanning Calorimetry (DSC)

In order to have complete data about both the physical and energy characteristics of materials, DSC is commonly used.[58]

Pure VRC thermogram showed a sharp endothermic peak at 129.2°C, consistent to its melting and its crystallinity (Figure 3C (i)).

Figures ii and iii show the thermal behavior of PLu F127 and CH, respectively, which appears as a sharp exothermic band at 55.4°C and 145.37°C, respectively due to the melting point of the corresponding polymer crystalline state.

However, DSC thermograms for physical mixtures of VRC with PLu F127 and CH do not shown any significant shift in the VRC exothermic peak where the peaks are shown at 48.76°C and 145.37°C, respectively (iv). Thus, the results of DSC thermograms confirmed that the physical mixtures of VRC and the two polymers used in Ns formulation were free from any chemical interaction. The reduction of the intensity of the VRC peak may be due to the dilution effect by the other used constituents.

Thermograms of F7 (vi) were similar to the thermograms of the respective polymer CH 143.58ºC with some shifting as VRC existed inside the polymers. On the other hand, it did not demonstrate the melting peak analogous to VRC; this result suggested that VRC had been highly encapsulated in the amorphous polymers with a less crystalline state, which was supported by x-ray analysis data.

The absence of the melting endotherm of VRC and shift of the endotherm of niosomal contents recommend the complete entrapment of the drug. This is in harmony with results recorded in a study,[59] where the absence of the melting endotherm of tretinoin and shifting of endotherm of the lipid bilayer of proniosomes was interpreted as a result of enhanced entrapment of the drug.

Physiochemical Evaluation of VRC-PNs Ocu

The prepared ocular inserts were characterized for their thickness 0.4–0.6 mm, average weight 0.1±0.02 g, drug content 98.2±1.1% as well as pH 6.8±0.3. These findings are optimum for ocular delivery.

In- Vitro Drug Release Study

The obtained curves in Figure 4 revealed that the complete, rapid release of VRC from the drug control suspension was accomplished within 2 h. On the contrary, the release of VRC from Ns displayed a biphasic release pattern that was firstly fast, 32.53±2.25% within the first half hour approximately, followed by a continuous release reaching 98.2±1.8% after 4 h. The initial burst effect could be linked to the drug portion reaching the outer surface of noisomes, while the second phase of the slow release of VRC out of the niosomal matrix was owing to diffusion. Adsorbed VRC would easily diffuse from the matrix, while VRC that had been incorporated into the nanoparticle core would be released over a prolonged period.[60]

The complete release of the pure drug from ocular inserts for 6 h was essential while the drug release from (VRC-Ns Ocu) was slower, taking a period of 8 h with lesser immediate burst effect than that of the niosomal suspension nearly 22.73±2.47% after half hour. This depicted that VRC was distributed and entrapped consistently into noisomes inside the ocusert matrix and gradually released out into the release medium that is in agreement with a study,[61] which demonstrated that

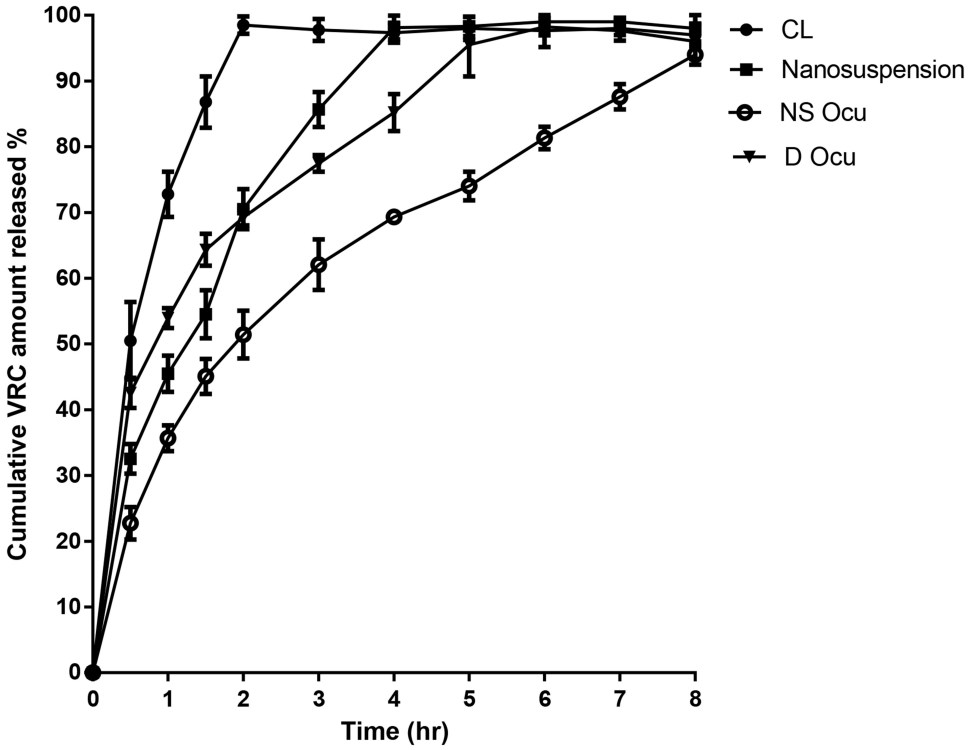


Figure 4 In-vitro release profile VRC formulae; (CL) control VRC suspension, (Ns) VRC nanosuspension, (Ns Ocu) niosomal drug-loaded ocusert, (D Ocu) free drug-loaded ocusert at pH 7.4.

viscosity-enhancing polymers like poloxamer and carbopol reduced the release rate of the drug via diffusion through gel matrix, but in our case, the viscosity-enhancing polymers were HPMC and carbopol $_{940}$.

Kinetics of the Drug Release

The gained fitting parameters are shown in Table 3. The tested formulation was best fixed with the Higuchi model with the uppermost regression coefficient (R^2) ranged between 0.69 & 0.98.

Supplementary analysis of our release data through Korsmeyer–Peppas was applied.[62] Korsmeyer n values of control suspension, F7 suspension and F7 ocular inserts formulations were established to be in the range of 0.48–0.56, which elucidated that the release process was a combination of diffusion and erosion mechanisms (anomalous non-Fickian transport). These results were found to be in agreement with those obtained by a study,[63] which reported that the kinetic modeling of in vitro release profiles of naproxen proniosomes could be described by the anomalous transport or non-Fickian diffusion mechanism through a biphasic release behavior as an initial fast release followed by a slower release with the Higuchi release mechanism. Also, another study,[64] demonstrated that the release of diosgenin from the prepared noisomes following diffusion and erosion ordered release

Table 3 Kinetic Analysis of Release Models of VRC from Control (CL) and the Prepared Selected Niosomal Formula F7 at pH 7.4 Containing 0.25% w/w Tween 80

Formula Code	Correlation Coefficient (R^2)			Release Mechanism	Korsmeyer – Peppas		Main Transport Mechanism
	Zero Order	First Order	Higuchi Model		R^2	N	
CL	0.4280	0.5554	0.6925	Diffusion	0.8643	0.53	Non-Fickian
F7 Susp	0.7380	0.6830	0.9180	Diffusion	0.9394	0.48	Non-Fickian
F7 Ocu	0.8874	0.9546	0.9899	Diffusion	0.9639	0.56	Non-Fickian
D Ocu	0.7261	0.8031	0.9225	Diffusion	0.9579	0.37	Fickian

Notes: D ocu, Ocular inserts containing free drug; R^2, Linear correlation coefficient; n, Diffusional exponent revealing of the drug release mechanism (slope).
Abbreviations: CL, control-free drug suspension; ocu, ocular insert.

progressions from the noisomes, thereby permitting the diffusion of diosgenin through the boundary.

Moreover, the free drug with an ocular insert n value 0.37 indicated that the release mechanism predominantly displayed diffusional and Fickian drug release.

Storage Stability Study

The stability results are listed in Table 4. No significant changes in evaluation parameters were recorded at the two storage temperatures throughout the storage period at each time interval. In contrast, upon comparison with the initial data after 5 months and more than that, a decline in the stability of the formula was observed more obviously at room temperature more than at a refrigerated temperature according to a significance of ($\rho < 0.05$) with a minor increase in particle size (252.58 ±5.71 nm), and a slight drug leakage with lowering of EE % (81.33±1.51%). Similar results were obtained in another study.[65]

Furthermore, the affinity for particles' accumulation and agglomeration may progress with their size expansion. Accordingly, the progressed VRC-loaded noisomal suspension (F7) is more stable at a refrigerated temperature (4±1°C) without the need of using the dried form.

Microbiological Study

Antifungal Susceptibility Testing

The results indicate that the voriconazole loaded niosomal formulations either as a suspension or as ocular inserts significantly hinder the proliferation of *Candida albicans* and *Aspergillus nidulans* in comparison with the formulations comprising just the free drug. The mean diameter of ZI with *Candida albicans* and *Aspergillus nidulans* is shown in Table 5. By experiment, we found insignificant growth retardation in the viscosity enhancer (HPMC) alone as it had no antifungal activity, suggesting that the fungal growth inhibition may be owing to the drug. VRC-PNs Ocu displayed superior antifungal activity against *Candida albicans* (more susceptible) than *Aspergillus nidulans*.[66] Therefore, HPMC promotes corneal drug permeation as manifested from the microbiological confirmation. VRC-PNs Ocu containing HPMC as a viscosity modifier slow down the growth of fungi. It may be assumed that the deposition of such adhesive polymers over the precorneal surface subsequently generates a concentration gradient for voriconazole permeation through cornea affording an extended contact stage.[67]

The mean inhibition zone ZI of formula (4) was 34.05 ±2.46 mm and 39.44±1.55 mm against *Candida albicans* and *Aspergillus nidulans*, respectively. This means that

Table 4 Stability Study Data of VRC- (F7) After Storage at Two Different Temperatures

Storage Time	Evaluation Parameters							
	Refrigeration Temperature (4±1°C)				Room Temperature			
	Particle Size (nm)	PDI	ZP (mV)	EE (%)	Particle Size (nm)	PDI	ZP (mV)	EE (%)
Initial	209.7±8.13	0.193±0.01	−33.5±1.85	87.4±2.55	209.7±8.13	0.193±0.01	−33.5±1.85	87.4±2.55
1 month	224.50±10.75	0.202±0.006	−33.23±0.153	86.06±0.21	225.6±10.26*	0.224±0.013	−32.50±0.78	86.10±0.27
2 months	235.93±2.49*	0.201±0.017	−33.43±1.07	84.63±0.57	238.33±2.08*	0.221±0.025	−30.56±0.55	85.66±0.49
3 months	238.10±1.32*	0.223±0.012	−30.70±0.53	83.80±0.99	240.33±1.53*	0.263±0.025	−28.96±0.45*	84.80±1.06
4 months	238.50±2.09*	0.210±0.026	−30.78±2.24	82.96±0.85	249.44±3.11*	0.285±0.008	−28.13±0.23*	83.86±1.03
5 months	244.50±3.08*	0.256±0.015	−29.10±0.89*	82.30±0.43*	250.07±4.10*	0.313±0.016*	−27.03±0.57*	82.00±2.27*
6 months	246.13±2.35*	0.263±0.032*	−29.10±0.095*	82.16±1.07*	252.58±5.71*	0.340±0.021*	−26.66±3.05*	81.33±1.51*

Notes: Each value represents the mean ± SD (n=3); *Significant at $\rho < 0.05$ monthly vs initial.
Abbreviations: VRC, voriconazole; NPs, nanoparticles; PDI, polydispersity index; EE, entrapment efficiency, ZP, Zeta potential.

Table 5 A Comparative Study of Antifungal Activity Against Two Species

Formula No.	Mean of Diameter of Zone of Inhibition (mm) ± SD *C. albicans*	Mean of Diameter of Zone of Inhibition (mm) ± SD *A. nidulans*
(1)	19.05±1.21	13.17±1.09
(2)	27.80±1.18	26.06±1.10
(3)	21.85±1.39	16.17±1.25
(4)	34.05±2.46	39.44±1.55

Notes: (1), free voriconazole suspension as control; (2), niosomal suspension of F7; (3), free drug-based ocuserts; (4), voriconazole niosomes based ocusert.

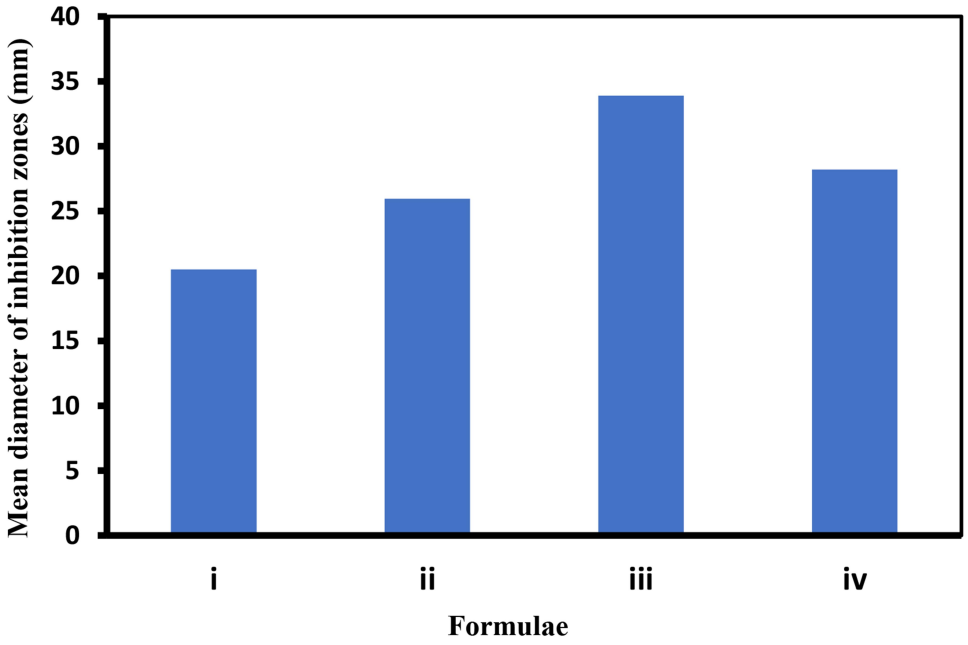


Figure 5 Bar graph representing the antifungal activity of voriconazole based niosomal ocuserts with different concentrations: 0.5% w/w (i), 0.75% w/w (ii), 1% w/w (iii), matched with natamycin 5% eye drops (iv) against *Candida albicans*.

VRC has more antifungal activity against *Aspergillus nidulans*. Also,[68] studies have found that the antifungal activity of voriconazole is greater than curcumin effect in case of *Aspergillus nidulans* which was emphasized by ZI diameter as voriconazole showed the minimum inhibitory zone of 20 mm whereas curcumin showed the zone of inhibition of only 10 mm diameter.

The explanation for the significant increase of ZI at ($\rho < 0.0001$) of F7 (4) compared with other three formulae is that ZI largely depends on the solubility and diffusion of the voriconazole through the agar media and exerts its antifungal effect against *Candida albicans* and *Aspergillus nidulans*.[69]

Comparative Antifungal Susceptibility Test

After a comparison between the mean values of inhibition zones of voriconazole niosomal based ocuserts with different concentrations and natamycin 5% eye drops (iv) against *Candida albicans* species, it can be observed from Figure 5 that formula (iii) which contains voriconazole based niosomal ocuserts in concentration 1% w/w exhibits higher antifungal activity against *Candida albicans* which is apparent through ZI of 33.9 mm that is very highly significant at $\rho < 0.0001$ compared with other formulae and is significantly different from control antifungal natamycin (iv). This superior performance over natamycin, signifies the effect of niosomal formulation across fungal cell membrane release with high quantities of VRC permitting significant inhibition of fungal growth.[70]

The obtained results revealed that the developed voriconazole based niosomal ocuserts in a concentration of 1% w/w is a promising formula and more efficient when compared to the other antifungal marketed drug.

Conclusion

Voriconazole was successfully prepared as proniosomes using coacervation phase separation method. VRC-PNs F7 are dispersed spherical particles with a nanoscopic diameter range, 200–247 nm and a narrow size distribution, suggesting facilitated access to eye tissues. The ocuserts provided prolonged release up to 8 h vs 2 h for free voriconazole. The microbiological studies showed that VRC-PNs Ocu (1% w/w) potentiate better antifungal activity compared to free voriconazole or natamycin eye drops. The ability of VRC to exert fungicidal activity might be triggered enhanced by its entrapment within noisomes. Actually, VRC-PNs Ocu deserve deep consideration for their potential future application as a hopeful nanoparticulate system for severe ocular antifungal infections.

Funding

This work was funded by the authors named in this article.

Disclosure

The authors report no conflicts of interest in this work. Authors declare no competing interests. Authors declare no competing financial interests.

References

1. Rowe-Rendleman CL, Durazo SA, Kompella UB, et al. Drug and gene delivery to the back of the eye: from bench to bedside. *Invest Ophthalmol Vis Sci*. 2014;55(4):2714–2730. doi:10.1167/iovs.13-13707
2. Patel A, Cholkar K, Agrahari V, Mitra AK. Ocular drug delivery systems: an overview. *World J Pharmacol*. 2013;2(2):47–64. doi:10.5497/wjp.v2.i2.47
3. Mun EA, Morrison PW, Williams AC, Khutoryanskiy VV. On the barrier properties of the cornea: a microscopy study of the penetration of fluorescently labeled nanoparticles, polymers, and sodium fluorescein. *Mol Pharm*. 2014;11(10):3556–3564. doi:10.1021/mp500332m
4. Huang D, Chen Y-S, Rupenthal ID. Overcoming ocular drug delivery barriers through the use of physical forces. *Adv Drug Deliv Rev*. 2018;126:96–112. doi:10.1016/j.addr.2017.09.008
5. Balguri SP, Adelli GR, Tatke A, Janga KY, Bhagav P, Majumdar S. Melt-cast noninvasive ocular inserts for posterior segment drug delivery. *J Pharm Sci*. 2017;106(12):3515–3523. doi:10.1016/j.xphs.2017.07.017
6. Abdelkader H, Ismail S, Hussein A, Wu Z, Al-Kassas R, Alany RG. Conjunctival and corneal tolerability assessment of ocular naltrexone niosomes and their ingredients on the hen's egg chorioallantoic membrane and excised bovine cornea models. *Int J Pharm*. 2012;432:1–10. doi:10.1016/j.ijpharm.2012.04.063
7. Bardania H, Tarvirdipour S, Dorkoosh F. Liposome-targeted delivery for highly potent drugs. *Artif Cells Nanomed Biotechnol*. 2017;45(8):1478–1489. doi:10.1080/21691401.2017.1290647
8. Allam A, Gamal SE, Naggar V. Formulation and evaluation of acyclovir niosomes for ophthalmic use. *Asian j Pharm Biol Res*. 2011;1(1):28–40.
9. Abdelbary GA, Amin MM, Zakaria MY. Ocular ketoconazole-loaded proniosomal gels: formulation, ex vivo corneal permeation and in vivo studies. *Drug Deliv*. 2017;24(1):309–319. doi:10.1080/10717544.2016.1247928
10. Lat A, Thompson III GR. Update on the optimal use of voriconazole for invasive fungal infections. *Infect Drug Resist*. 2011;4:43–53. doi:10.2147/IDR.S12714
11. Siafaka PI, Üstündağ Okur N, Mone M, et al. Two different approaches for oral administration of voriconazole loaded formulations: electrospun fibers versus β-cyclodextrin complexes. *Int J Mol Sci*. 2016;17(3):282. doi:10.3390/ijms17030282
12. Sun X, Yu Z, Cai Z, Yu L, Lv Y. Voriconazole composited polyvinyl alcohol/hydroxypropyl-β-cyclodextrin nanofibers for ophthalmic delivery. *PLoS One*. 2016;11(12):1–18. doi:10.1371/journal.pone.0167961
13. Gupta S, Shrivastava RM, Tandon R, Gogia V, Agarwal P, Satpathy G. Role of voriconazole in combined acanthamoeba and fungal corneal ulcer. *Cont Lens Anterior Eye*. 2011;34(6):287–289. doi:10.1016/j.clae.2011.06.004
14. Pahuja P, Kashyap H, Pawar P. Design and evaluation of HP-β-CD based voriconazole formulations for ocular drug delivery. *Curr Drug Deliv*. 2014;11(2):223–232. doi:10.2174/1567201810666131224105205
15. Pawar P, Kashyap H, Malhotra S, Sindhu R. Hp–CD-voriconazole in situ gelling system for ocular drug delivery: in vitro, stability, and antifungal activities assessment. *Biomed Res Int*. 2013;2013. doi:10.1155/2013/341218
16. Kumar R, Sinha VR. Preparation and optimization of voriconazole microemulsion for ocular delivery. *Colloids Surf B Biointerfaces*. 2014;117:82–88. doi:10.1016/j.colsurfb.2014.02.007
17. de Sá FAP, Taveira SF, Gelfuso GM, et al. Liposomal voriconazole (VOR) formulation for improved ocular delivery. *Colloids Surf B Biointerfaces*. 2015;133:331–338. doi:10.1016/j.colsurfb.2015.06.036
18. Shukr MH. Novel in situ gelling ocular inserts for voriconazole-loaded niosomes: design, in vitro characterisation and in vivo evaluation of the ocular irritation and drug pharmacokinetics. *J Microencapsul*. 2016;33(1):71–79. doi:10.3109/02652048.2015.1128489
19. Amorós-Reboredo P, Bastida-Fernandez C, Guerrero-Molina L, Soy-Muner D, Carmen L-C. Stability of frozen 1% voriconazole ophthalmic solution. *Am J Health Syst Pharm*. 2015;72(6):479–482. doi:10.2146/ajhp140127
20. Gower EW, Keay LJ, Oechsler RA, et al. Trends in fungal keratitis in the United States, 2001 to 2007. *Ophthalmology*. 2010;117(12):2263–2267. doi:10.1016/j.ophtha.2010.03.048
21. Parthibarajan R, Pradeep Kumar S, Shankar NG, et al. Design and invitro evaluation of voriconazole niosomes. *Int J Pharma and Pharmaceu Sci*. 2013;5(3):604–611.
22. He D, Hao J, Gao S, et al. Etiological analysis of fungal keratitis and rapid identification of predominant fungal pathogens. *Mycopathologia*. 2016;181(1–2):75–82. doi:10.1007/s11046-015-9950-x
23. Mahmoudi S, Masoomi A, Ahmadikia K, et al. Fungal keratitis: an overview of clinical and laboratory aspects. *Mycoses*. 2018;61(12):916–930. doi:10.1111/myc.12822
24. Al-Badriyeh D, Neoh CF, Stewart K, Kong DC. Clinical utility of voriconazole eye drops in ophthalmic fungal keratitis. *Clin Ophthalmol*. 2010;4:391. doi:10.2147/opth.s6374
25. Abd El Alim M, Abdel Halim RM, Habib SA. Comparison of broth micro dilution and disk diffusion methods for susceptibility testing of dermatophytes. *Egypt J Hosp*. 2017;69(2):1923–1930. doi:10.12816/0040624
26. Perrett S, Golding M, Williams WP. A simple method for the preparation of liposomes for pharmaceutical applications: characterization of the liposomes. *J Pharm Pharmacol*. 1991;43(3):154–161. doi:10.1111/j.2042-7158.1991.tb06657.x
27. Fouda NH, Abdelrehim RT, Hegazy DA, Habib BA. Sustained ocular delivery of Dorzolamide-HCl via proniosomal gel formulation: in-vitro characterization, statistical optimization, and in-vivo pharmacodynamic evaluation in rabbits. *Drug Deliv*. 2018;25(1):1340–1349. doi:10.1080/10717544.2018.1477861
28. Vora B, Khopade AJ, Jain N. Proniosome based transdermal delivery of levonorgestrel for effective contraception. *J Control Release*. 1998;54(2):149–165. doi:10.1016/S0168-3659(97)00100-4
29. Habib BA, Sayed S, Elsayed GM. Enhanced transdermal delivery of ondansetron using nanovesicular systems: fabrication, characterization, optimization and ex-vivo permeation study-Box-Cox transformation practical example. *Eur J Pharm Sci*. 2018;115:352–361. doi:10.1016/j.ejps.2018.01.044
30. Fahmy AM, El-Setouhy DA, Ibrahim AB, Habib BA, Tayel SA, Bayoumi NA. Penetration enhancer-containing spanlastics (PECSs) for transdermal delivery of haloperidol: in vitro characterization, ex vivo permeation and in vivo biodistribution studies. *Drug Deliv*. 2018;25(1):12–22. doi:10.1080/10717544.2017.1410262
31. Sharma D, Tyagi S, Kumar B. Novel approaches of treatment via ocusert drug delivery. *Asian J Nanosci Mater*. 2019;2:356–366. doi:10.26655/AJNANOMAT.2019.2.3.9
32. Teodorescu F, Queniat G, Foulon C, et al. Transdermal skin patch based on reduced graphene oxide: a new approach for photothermal triggered permeation of ondansetron across porcine skin. *J Control Release*. 2017;245:137–146. doi:10.1016/j.jconrel.2016.11.029

33. Higuchi T. Mechanism of sustained-action medication. Theoretical analysis of rate of release of solid drugs dispersed in solid matrices. *J Pharm Sci*. 1963;52(12):1145–1149. doi:10.1002/jps.2600521210
34. Ritger PL, Peppas NA. A simple equation for description of solute release I. Fickian and non-fickian release from non-swellable devices in the form of slabs, spheres, cylinders or discs. *J Control Release*. 1987;5(1):23–36. doi:10.1016/0168-3659(87)90034-4
35. Goswami S, Pathak D. Niosomes-a review of current status and application. *World J Pharm Pharm Sci*. 2017;594–615. doi:10.20959/wjpps20176-9296
36. Fonzi WA, Irwin MY. Isogenic strain construction and gene mapping in Candida albicans. *Genetics*. 1993;134(3):717–728.
37. Wayne PA. *Performance Standards for Antimicrobial Disk Susceptibility Tests*. Clinical and Laboratory Standards Institute, CLSI,(2009); 2010.
38. Kumar GP, Rajeshwarrao P. Nonionic surfactant vesicular systems for effective drug delivery—an overview. *Acta Pharm Sin B*. 2011;1(4):208–219. doi:10.1016/j.apsb.2011.09.002
39. Bnyan R, Khan I, Ehtezazi T, et al. Surfactant effects on lipid-based vesicles properties. *J Pharm Sci*. 2018;107(5):1237–1246. doi:10.1016/j.xphs.2018.01.005
40. Bachhav AA. Proniosome: a novel non-ionic provesicules as potential drug carrier. *Asian J Pharm*. 2016;10(03). doi:10.1016/j.xphs.2018.01.005
41. Ramadan AA, Eladawy SA, El-Enin ASMA, Hussein ZM. Development and investigation of timolol maleate niosomal formulations for the treatment of glaucoma. *J Pharm Investig*. 2020;50(1):59–70. doi:10.1007/s40005-019-00427-1
42. Zaki AM, Carbone P. How the incorporation of Pluronic block copolymers modulates the response of lipid membranes to mechanical stress. *Langmuir*. 2017;33(46):13284–13294. doi:10.1021/acs.langmuir.7b02244
43. Gharbavi M, Amani J, Kheiri-Manjili H, Danafar H, Sharafi A. Niosome: a promising nanocarrier for natural drug delivery through blood-brain barrier. *Adv Pharmacol Pharm Sci*. 2018;2018. doi:10.1155/2018/6847971
44. Rawat A, Kumar MS, Khurana B, Mahadevan N. Proniosome gel: a novel topical delivery system. *Int J Rec Adv Pharm Res*. 2011;3(1):1–10.
45. Yadav K, Yadav D, Saroha K, Nanda S, Mathur P, Syan N. Proniosomal Gel: a provesicular approach for transdermal drug delivery. *Der Pharmacia Lettre*. 2010;2(4):189–198.
46. Moghddam SRM, Ahad A, Aqil M, Imam SS, Sultana Y. Formulation and optimization of niosomes for topical diacerein delivery using 3-factor, 3-level Box-Behnken design for the management of psoriasis.. *Mater Sci Eng C*. 2016;69:789–797. doi:10.1016/j.msec.2016.07.043
47. Kamaleddin MA. Nano-ophthalmology: applications and considerations. *Nanomedicine: NBM*. 2017;13(4):1459–1472. doi:10.1016/j.nano.2017.02.007
48. Chauhan S, Batra S. Development and in vitro characterization of nanoemulsion embedded thermosensitive in-situ ocular gel of diclofenac sodium for sustained delivery. *Int J Pharm Sci Res*. 2018;9(6):2301–2314.
49. Khosa A, Reddi S, Saha RN. Nanostructured lipid carriers for site-specific drug delivery. *Biomed Pharmacother*. 2018;103:598–613. doi:10.1016/j.biopha.2018.04.055
50. Clayton KN, Salameh JW, Wereley ST, Kinzer-Ursem TL. Physical characterization of nanoparticle size and surface modification using particle scattering diffusometry. *Biomicrofluidics*. 2016;10(5):05410. doi:10.1063/1.4962992
51. Aneesha P, Ghate MV, Narayan R, Abraham S. Proniosomes as a novel drug carrier for the delivery of ketoprofen. *Adv Sci Lett*. 2017;23(3):1858–1863. doi:10.1166/asl.2017.8496
52. Mori NM, Patel P, Sheth NR, Rathod LV, Ashara KC. Fabrication and characterization of film-forming voriconazole transdermal spray for the treatment of fungal infection. *Bull Fac Pharm Cairo Univ*. 2017;55(1):41–51. doi:10.1016/j.bfopcu.2017.01.001
53. Dewan M, Sarkar G, Bhowmik M, et al. Effect of gellan gum on the thermogelation property and drug release profile of Poloxamer 407 based ophthalmic formulation. *Int J Biol Macromol*. 2017;102:258–265. doi:10.1016/j.ijbiomac.2017.03.194
54. Madni A, Rahim MA, Mahmood MA, et al. Enhancement of dissolution and skin permeability of pentazocine by proniosomes and niosomal gel. *AAPS PharmSciTech*. 2018;19(4):1544–1553. doi:10.1208/s12249-018-0967-6
55. Khare A, Singh I, Pawar P, Grover K. Design and evaluation of voriconazole loaded solid lipid nanoparticles for ophthalmic application. *J Drug Deliv*. 2016;1–11. doi:10.1155/2016/6590361
56. Sezgin-Bayindir Z, Yuksel N. Investigation of formulation variables and excipient interaction on the production of niosomes. *AAPS PharmSciTech*. 2012;13(3):826–835. doi:10.1208/s12249-012-9805-4
57. De Melo PN, De Caland LB, Fernandes-Pedrosa MF, Da Silva-júnior AA. Designing and monitoring microstructural properties of oligosaccharide/co-solvent ternary complex particles to improve benznidazole dissolution. *J Mater Sci*. 2018;53(4):2472–2483. doi:10.1007/s10853-017-1720-3
58. El-Badry M, Hassan MA, Ibrahim MA, Elsaghir H. Performance of poloxamer 407 as hydrophilic carrier on the binary mixtures with nimesulide. *Farmacia*. 2013;61(6):1137–1150.
59. Rahman SA, Abdelmalak NS, Badawi A, Elbayoumy T, Sabry N, Ramly AE. Formulation of tretinoin-loaded topical proniosomes for treatment of acne: in-vitro characterization, skin irritation test and comparative clinical study. *Drug Deliv*. 2015;22(6):731–739. doi:10.3109/10717544.2014.896428
60. Liu R, Wang S, Fang S, et al. Liquid crystalline nanoparticles as an ophthalmic delivery system for tetrandrine: development, characterization, and in vitro and in vivo evaluation. *Nanoscale Res. Lett*. 2016;11(1):254. doi:10.1186/s11671-016-1471-0
61. Akhtar N, Singh RK, Pathak K. Exploring the potential of complex-vesicle based niosomal ocular system loaded with azithromycin: development of in situ gel and ex vivo characterization. *Pharm Biomed Res*. 2017;3(1):22–33. doi:10.18869/acadpub.pbr.3.1.22
62. Korsmeyer RW, Gurny R, Doelker E, Buri P, Peppas NA. Mechanisms of solute release from porous hydrophilic polymers. *Int J Pharm*. 1983;15(1):25–35. doi:10.1016/0378-5173(83)90064-9
63. Mohanty D, Rani MJ, Akiful Haque M, et al. Preparation and evaluation of transdermal naproxen niosomes: formulation optimization to preclinical anti-inflammatory assessment on murine model. *J Liposome Res*. 2019;1–11. doi:10.1080/08982104.2019.1652646
64. Hajizadeh MR, Parvaz N, Barani M, et al. Diosgenin-loaded niosome as an effective phytochemical nanocarrier: physicochemical characterization, loading efficiency, and cytotoxicity assay. *DARU J Pharm Sci*. 2019;27(1):329–339. doi:10.1007/s40199-019-00277-0
65. Shrivastava B. Topical combination delivery of benzoyl peroxide and adapalene niosomal gel for acne treatment. *Asian J Pharm*. 2019;13(04).
66. Veloso DF, Benedetti NI, Ávila RI, et al. Intravenous delivery of a liposomal formulation of voriconazole improves drug pharmacokinetics, tissue distribution, and enhances antifungal activity. *Drug Deliv*. 2018;25(1):1585–1594. doi:10.1080/10717544.2018.1492046
67. Malhotra S, Khare A, Grover K, Singh I, Pawar P. Design and evaluation of voriconazole eye drops for the treatment of fungal keratitis. *Int J Pharm*. 2014. doi:10.1155/2014/490595
68. Gitika A, Mishra R, Panda SK, Mishra C, Ranjan PR, hoo S. Evaluation of antifungal activity of curcumin against Aspergillus flavus. *Int J Curr Microbiol Appl Sci*. 2019;8(7):2323–2329. doi:10.20546/ijcmas.2019.807.284
69. Sharma A, Sharma K. Should solubility and zone of inhibition be the only criteria for selection of solvent in antimicrobial assay. *Adv Biol Res*. 2011;5(5):241–247.
70. Ling X, Huang Z, Wang J, et al. Development of an itraconazole encapsulated polymeric nanoparticle platform for effective antifungal therapy. *J Mater Chem B*. 2016;4(10):1787–1796. doi:10.1039/C5TB02453F

International Journal of Nanomedicine Dovepress

Publish your work in this journal

The International Journal of Nanomedicine is an international, peer-reviewed journal focusing on the application of nanotechnology in diagnostics, therapeutics, and drug delivery systems throughout the biomedical field. This journal is indexed on PubMed Central, MedLine, CAS, SciSearch®, Current Contents®/Clinical Medicine, Journal Citation Reports/Science Edition, EMBase, Scopus and the Elsevier Bibliographic databases. The manuscript management system is completely online and includes a very quick and fair peer-review system, which is all easy to use. Visit http://www.dovepress.com/testimonials.php to read real quotes from published authors.

Submit your manuscript here: https://www.dovepress.com/international-journal-of-nanomedicine-journal